Quaternary Research 73 (2010) 84–95

Contents lists available at ScienceDirect

Quaternary Research

journal homepage: www.elsevier.com/locate/yqres

Variations in sediment yield over the advance and retreat of a calving glacier, Laguna San Rafael, North Patagonian Icefield

Michèle Koppes [a,*], Richard Sylwester [b], Andres Rivera [c,d], Bernard Hallet [e]

[a] Department of Geography, 1984 West Mall, University of British Columbia, Vancouver, BC, Canada V6T 1Z2
[b] Golder Associates Inc., Redmond, WA 98052, USA
[c] Centro de Estudios Cientificos, Valdivia, Chile
[d] Departamento de Geografía, Universidad de Chile, Santiago, Chile
[e] Department of Earth and Space Sciences and Quaternary Research Center, University of Washington, Seattle, WA 98195-1310, USA

ARTICLE INFO

Article history:
Received 10 September 2008
Available online 30 September 2009

Keywords:
Sediment yields
Subaqueous geomorphology
Glacial erosion rates
Little Ice Age
Acoustic reflection profiles
North Patagonia

ABSTRACT

Bathymetric and sub-bottom acoustic data were collected in Laguna San Rafael, Chile, to determine sediment yields during the Little Ice Age advance and subsequent retreat of San Rafael Glacier. The sediment volumes and subaqueous landforms imaged are used to interpret the proglacial dynamics and estimate erosion rates from a temperate tidewater glacier over a complete advance–retreat cycle. Sediment yields from San Rafael Glacier averaged 2.7×10^7 m^3/a since the end of the Little Ice Age, circa AD 1898, corresponding to average basin-wide erosion rates of 23 ± 9 mm/a; the highest erosion rates, 68 ± 23 mm/a, occurred at the start of the retreat phase, and have since been steadily decreasing. Erosion rates were much lower during glacial advance, averaging at most 7 mm/a, than during retreat. Such large glacial sediment yields over two centuries of advance and retreat suggest that the contribution of sediments stored subglacially cannot account for much of the sediment being delivered to the terminus today. The detailed sub-bottom information of a proglacial lagoon yields important clues as to the timing of erosion, deposition and transfer of glacigenic sediments from orogens to the continental shelves, and the influence of glacier dynamics on this process.

Introduction

The rich sedimentary records found throughout the mid- to high-latitude continental margins are vital for deciphering climate change and assess the relationship among climate, erosion and landscape evolution. The change to a cool, variable climate beginning ~2–4 Ma and the onset of late Cenozoic glaciation coincided with a global increase in sedimentation (Hay et al., 1988; Peizhen et al., 2001), including the deposition of extensive glaciomarine sedimentary sequences on continental shelves from the Antarctic to the high Arctic (e.g., Vorren et al., 1991; Lagoe et al., 1993; Bart and Anderson, 1995; Elverhøi et al., 1995). These glaciomarine sequences reveal a complex history of Quaternary climate change recorded in sediment accumulation rates that reflect climate-driven changes in sediment yields from the adjacent glaciers and ice sheets.

Deciphering such climate history from the glacial sediment record is complex. It is limited by our ability to link the spatio-temporal variation in glacial sediment yields to the climate dynamics that drive ice-sheet growth and erosion, as well as to variations in the transfer and deposition of sediment from glaciers to the continental shelves. Calving glaciers in particular have a complex relationship with climate change, largely due to their sensitivity to non-climatic factors such as water depth or terminus topography. These factors can also control the rate of ice loss at the glacier terminus, which has been observed to relate directly to ice velocity (Van der Veen, 2002), and by extension to sediment yields (e.g., Humphrey and Raymond, 1994). Calving glaciers drain many of the remaining icefields on Earth, therefore understanding the drivers influencing glacial sediment yields and the transfer and reworking of glacial sediments from calving glaciers over both short- and long-term glacial cycles is needed.

Real-time observations of sediment delivery to the termini of glaciers and the ice dynamics that control the rate of sediment production are needed to fully address the relationship between climatic and non-climatic forcings and glacial sediment yields. Observing the patterns of sediment accumulation at the front of a calving glacier is particularly challenging due to the inherently dangerous conditions at the ice margin. A few studies have succeeded in using ice-penetrating radar near the calving front to image the evolving subglacial surface and bedforms and to relate them to dynamics near the terminus (e.g., Motyka et al., 2006). However, heavy crevassing and significant englacial water common to the terminal zone of glaciers can disrupt and attenuate the radar signal resulting in limited subsurface penetration and/or poor quality

* Corresponding author. Fax: +1 604 822 6150.
E-mail address: koppes@geog.ubc.ca (M. Koppes).

0033-5894/$ – see front matter
doi:10.1016/j.yqres.2009.07.006

records. Therefore, geomorphologists are most often left to decipher subglacial and near-glacial conditions from the landforms that postdate ice retreat. Unfortunately, the morphology of these landforms only reflects the final phase of the advance/retreat cycle. Imaging what is below the sediment surface is hence invaluable, and provides the best understanding of the history of the sediment accumulation and the timing of its deposition in relation to the terminus.

This study provides a history of the Little Ice Age extent and sediment yield from San Rafael Glacier, Chile. We describe the subaqueous morphology, structural forms and sediment accumulation rates in Laguna San Rafael since the last substantive advance of the San Rafael Glacier, based on sub-bottom acoustic profiles of the lagoon sediments. The history of San Rafael Glacier is of special interest because it is a) the most equatorial tidewater glacier in the world (46°40′ S, 73°49′ W), b) one of the fastest flowing glaciers worldwide (Kondo and Yamada, 1988; Rignot et al., 1996, 2003), and c) drains almost 20% of the Hielo Patagonico Norte (North Patagonian Icefield), an ice cap covering ~3953 km^2 that contains some of the last significant stores of temperate ice on Earth (Rivera et al., 2007). Located in the midst of the Southern Westerlies, a zone of strong westerly winds, mild temperatures year-round and high precipitation, San Rafael Glacier was particularly sensitive to latitudinal changes in temperature and atmospheric circulation in the recent past (Glasser et al., 2004; Mayr et al., 2007). Significant fluctuations of the terminus and of sediment delivery to the glacier front have occurred over recent geologic time. The sediments deposited and sculpted by the glacier leave a rich record of the interaction of the glacier and its bed near the shifting ice front, as well as a history of the erosion and delivery of sediments generated from the entire glacier basin. The distribution of sediments in the lagoon in front of the glacier provides critical clues as to how the sediment yield from a glacier may vary throughout a cycle of advance and retreat, clues needed to interpret the climate history from the Quaternary glacimarine sediment package located just offshore.

Historical glacier fluctuations in Laguna San Rafael

San Rafael Glacier terminates in a brackish lagoon, Laguna San Rafael which is encircled by the Tempanos Moraine, a massive terminal moraine that traces a 35 km-long arc at 15–30 m above sea level (masl) containing the lagoon (Fig. 1). The moraine is a complex, multi-crested ridge formed during the Holocene by one or more advances of the glacier (Glasser et al., 2006). To the northwest it is breached by the Rio Tempanos (Iceberg River), a shallow river (<12 m deep in the thalweg) that connects the lagoon to the Golfo Elefantes and the ocean. This allows seawater to enter the lagoon, but prevents any sediment from exiting the lagoon except infrequently as ice-rafted debris. In the past, the lagoon may have been connected to the ocean by a second shallow river draining to the south; this outlet has since been blocked by an advance of neighboring San Quintin Glacier. The eastern edge of the lagoon is bounded by the front range of the Andes at the Liquiñe-Ofqui Mega Thrust (Cembrano et al., 1996). The lagoon therefore acts as an efficient trap for sediments delivered by the glacier. Furthermore, the relatively still waters of the lagoon and shallow outlet to the Rio Tempanos have acted to effectively preserve subaqueous stratigraphic features.

San Rafael Glacier has one of the longest documented fluctuation history of any glacier in southern South America. Early historical records suggest that in AD 1675 the glacier was less extensive than today and possibly terminated on land (Araneda et al., 2007). It started to advance into Laguna San Rafael between AD 1742 and 1766, when the ice front advanced into water deep enough to initiate calving (Casassa and Marangunic, 1987; Araneda et al., 2007). The glacier reached its Little Ice Age (LIA) maximum sometime around the middle of the 19th century (Heusser, 1960), about the same time as several glaciers of the North and South Patagonian Icefields formed prominent terminal moraines (summarized in Glasser et al., 2004). Prior studies have speculated that the glacier did not cross the lagoon completely during this LIA advance, but was restricted to a piedmont lobe protruding into the center of the lagoon by rapid calving into deep water (Warren, 1993; Glasser et al., 2005). The first precise description of the piedmont-type ice front was recorded by Comandante Enrique Simpson in AD 1871, who was surveying Laguna San Rafael for a potential inland waterway through the Patagonian fjords. Simpson described the terminus as extending 8 km from the Andean front, ending 3 km from the arcuate moraine that bounded the lagoon (Simpson, 1875; Casassa and Marangunic, 1987) (see Fig. 2). The ice front was in the same approximate location when Dr. Hans Steffen visited Laguna San Rafael in December 1898 (Steffen, 1910). Based on dates from vegetation found at the prominent trimline along the rangefront (Lawrence and Lawrence, 1959; Winchester and Harrison, 1996) the start of the latest retreat phase of the glacier from its LIA maximum began sometime around Dr. Steffen's visit. The terminus then retreated erratically, reaching the vicinity of the now-destroyed hotel and forming a recessional moraine in AD 1910 (Glasser et al., 2005). Over 2 km of retreat occurred between AD 1905 and 1921, and another 1.8 km between AD 1921 and 1935 (Masiokas et al., 2009), followed by a standstill that lasted until around 1959 (Lawrence and Lawrence, 1959). Oblique aerial photos taken by the U.S. Air Force in 1945 captured the terminus position during this standstill. Since the early 1960s, retreat of the ice front has continued to its present position 3 km east of the rangefront (Fig. 2).

The Tempanos Moraine was deposited on a pre-existing outwash plain of the last major glacial advance, the Llanquihue event, which occurred 14–34 ka (Mercer, 1976). During that advance, glaciers occupied almost the entire continental margin out to the shelf break south of 40° S. Around 11 ka, the icefield shrank back to its approximate present extent, and the San Rafael Glacier has since fluctuated within the area of the lagoon (Winchester and Harrison, 1996). The age of the Tempanos Moraine is debated, ranging from 6850 ± 200 ^{14}C yr BP (Heusser, 1960) to 3600 ^{14}C yr BP (Muller, 1960). Dating has been problematic because of the complex sedimentology, the result of the terminus occupying the same position more than once during the Holocene, with the glacier reworking older sediments and redepositing them in the terminal moraine during each readvance (Glasser et al., 2005, 2006). Nonetheless, we are assuming that any unconsolidated sediments currently filling the lagoon were delivered by the San Rafael Glacier since it last advanced to the lagoon's edge at some time during the late Holocene.

Methods

We collected acoustic reflection profiles in the Laguna San Rafael in April 2006 aboard the MV Petrel IV, the national park boat owned and operated by the Chilean National Forestry Service. The subsurface reflection data were obtained using a Datasonics Bubble Pulser and 4 m hydrophone and processed with a GeoAcoustic amplifier. Penetration depth of the acoustic signal exceeded 200 m in the soft glaciolacustrine sediments and imaged several acoustic reflectors that represent different glacial facies. The acoustic signals were digitally imported into the SonarWiz-SBP software suite for post-processing and analysis. Water depths were calculated using a seismic velocity of 1460 m/s for brackish water, measured from a series of conductivity/temperature/depth (CTD) casts taken in the center of the lagoon, and verified using a Lowrance 18-C depth profiler. The thickness of sedimentary facies were estimated by converting the two-way travel time of the acoustic signal to sediment depth assuming a seismic compressional velocity in glacimarine sediments of 1680–1740 m/s (Stoker et al., 1997). This conversion results in a time scale of 100 ms being equal to 84–87 m of sediment. Vertical resolution was 1 ms ~8 m). The thickness of postglacial sediment was

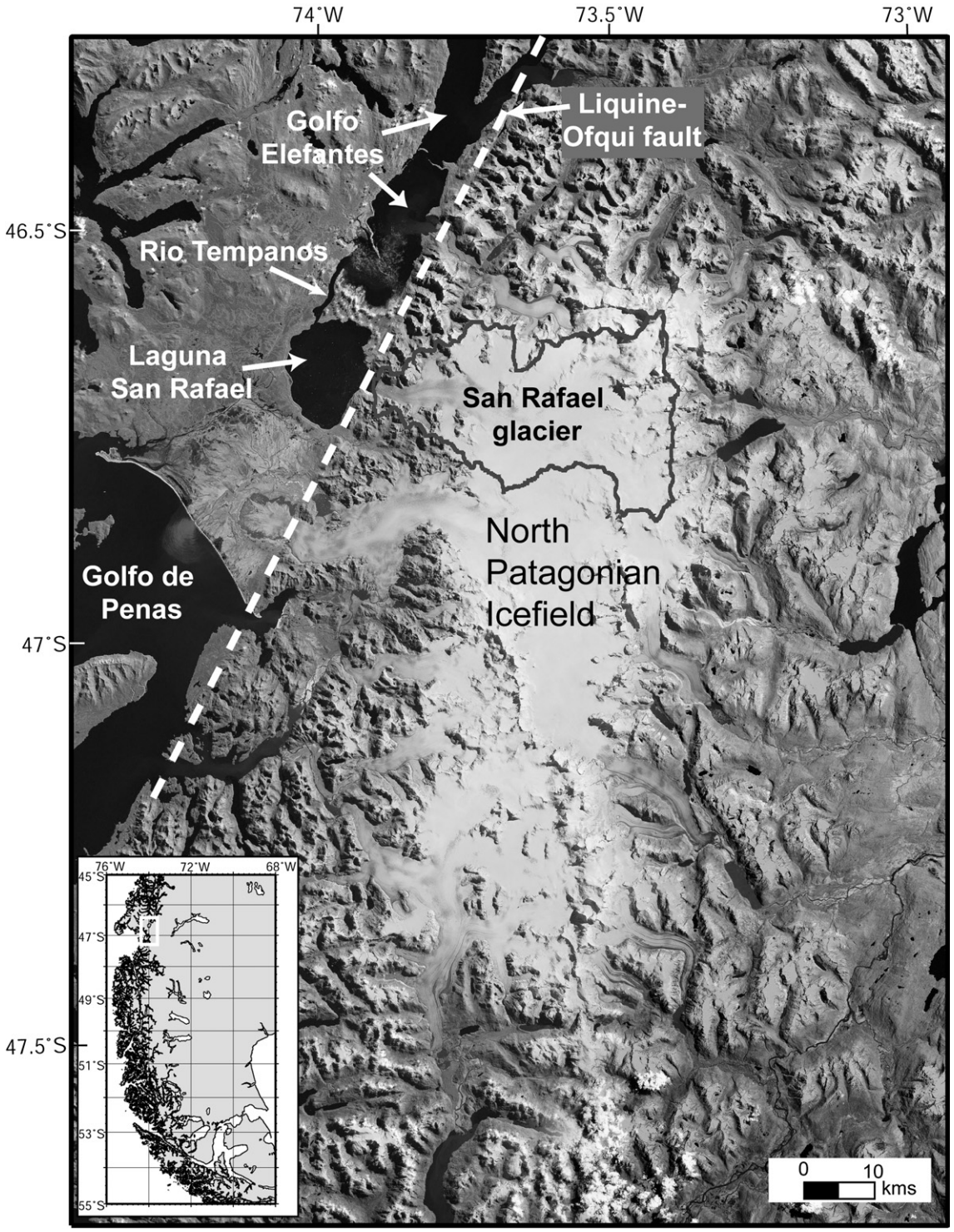

Figure 1. Location map of Laguna San Rafael, including the major geographic features of the region. The lagoon is bounded by the arcuate Tempanos Moraine to the west and the Andean rangefront to the east. The basin of the San Rafael Glacier is outlined in dark grey.

measured from the deepest, most prominent reflector which was interpreted to be the top of bedrock (east of the rangefront) or of deformable lacustrine sediment compacted by glacier overriding during the last LIA advance (west of the rangefront). The tracklines, water depth and sediment thicknesses were imported into ArcGIS and gridded using cubic-spline interpolation and a kriging function to estimate the bathymetry and sediment volumes between ship tracks (Fig. 3A). Errors in calculating total sediment volume in the lagoon using this gridding method were propagated using leave-one-out cross-validation, wherein several tracklines were removed from the dataset and the sediment volumes regridded and compared to the full dataset to estimate errors from the gridding process. The maximum estimated error using our grid interpolation was 22% of sediment thickness (see Koppes, 2007 for a full description of methods used).

We calculated the average annual sediment yield from San Rafael Glacier from the start of its current retreat phase sequentially through the early part of the 20th century, using the AD 1871, 1905, 1921, 1935 and 1959 terminus positions previously mapped by Warren (1993),

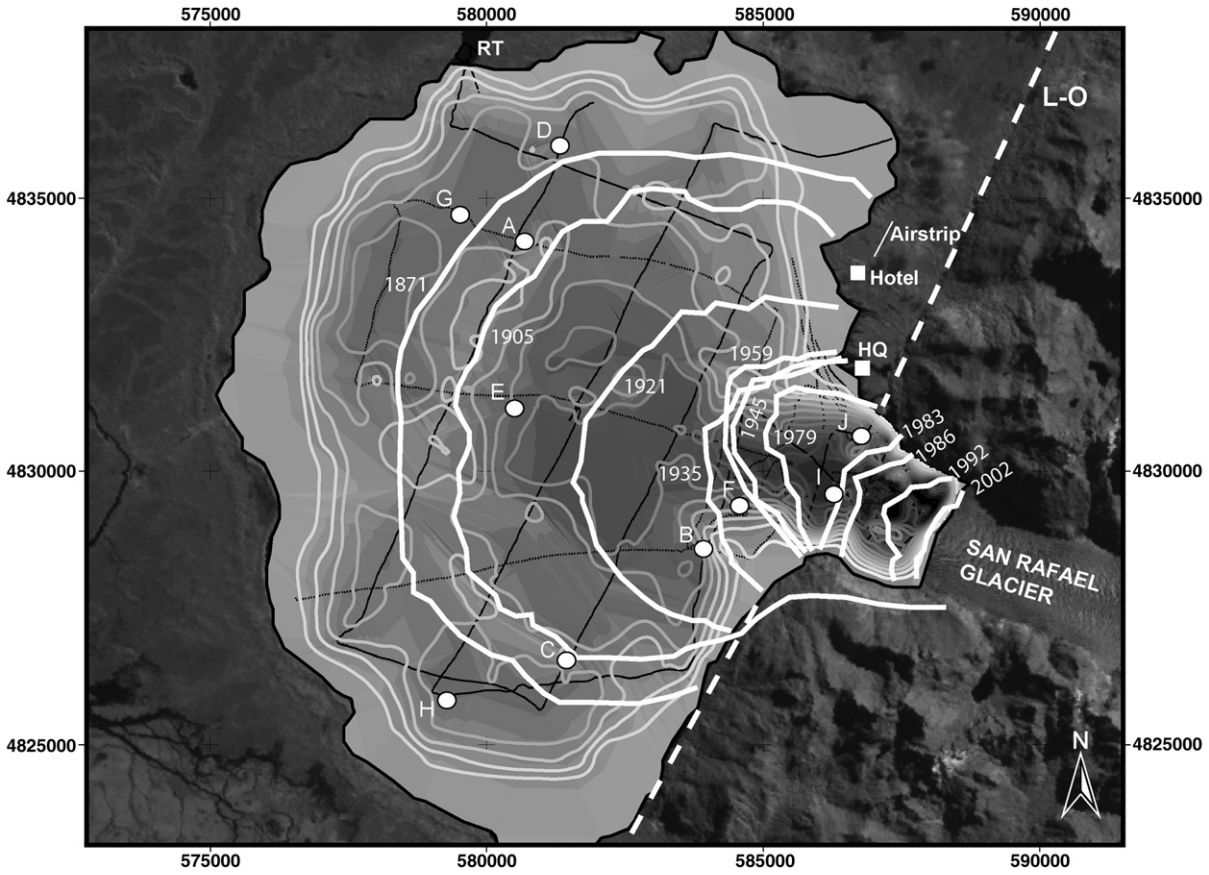

Figure 2. Bathymetry of Laguna San Rafael, including tracklines from the acoustic profiles (black lines), the location and dates of documented ice front positions (in white) and the location of seismic images A–J in Figures 4–6. Map grid is in UTM zone 18S. Contour interval is 20 m.

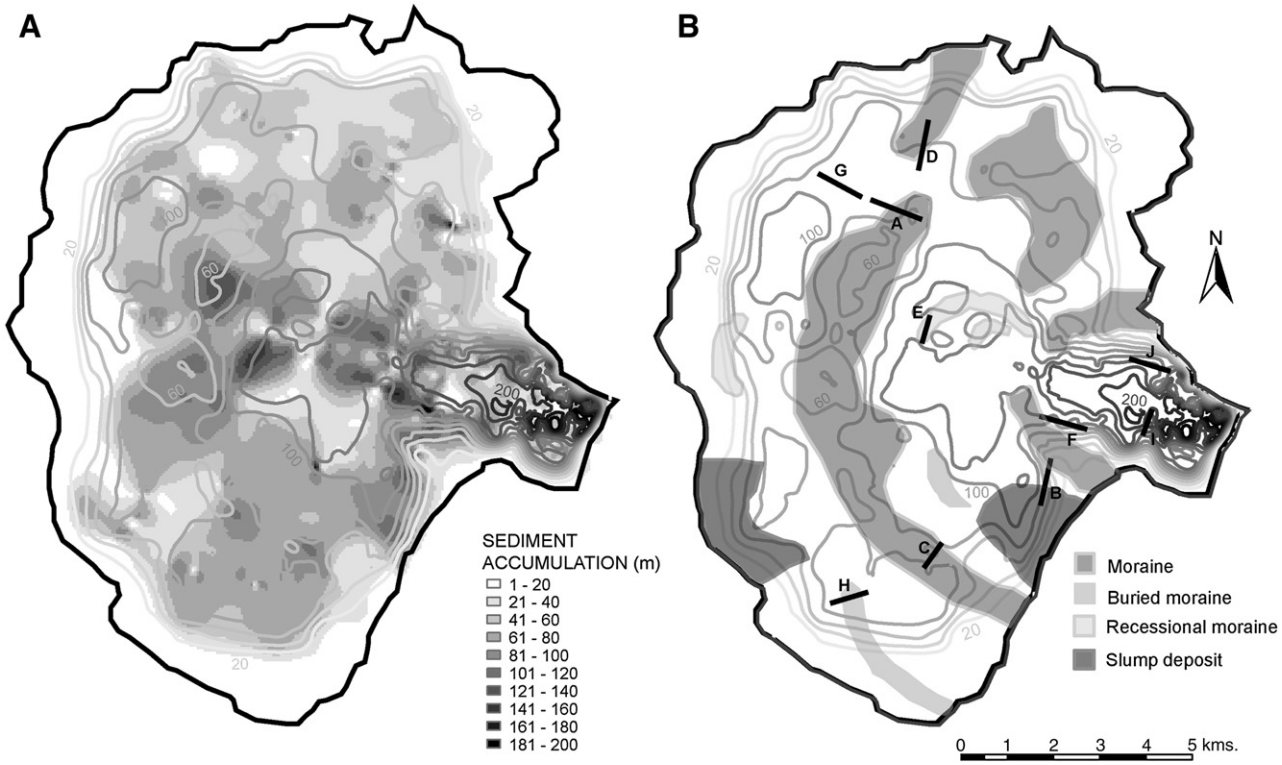

Figure 3. (A) Total sediment accumulation in Laguna San Rafael from the most recent advance and retreat, including contours of subaqueous bathymetry. (B) Distribution of the major subaqueous landforms in the lagoon, with locations of the seismic profiles in Figures 4–6. Contour interval is 20 m.

Glasser et al. (2006) and Araneda et al. (2007). We estimate the uncertainty in determining historical terminus positions from these maps is close to 18% of the lagoon area, particularly for the earliest positions. The average annual sediment yield was computed by dividing the volume of sediment between these terminus positions by the corresponding time interval. This approach assumes that a) all unconsolidated glaciolacustrine sediments were deposited beyond the calving front (i.e., no subglacial deposition), and b) there has been negligible postdepositional reworking and transport by turbidity currents and subaqueous mass movements beyond the proximal zone, ~2 km from the calving front. In using this approach, any sediment spill over the earlier terminus position would introduce compensating errors, reducing the average sediment yield for that time interval, while increasing it during the preceding time period. Combining the gridding uncertainties with the uncertainties in mapping the exact position of the terminus over time, we estimate a maximum error of 40% in our sediment yield calculations.

To convert sediment yields to the average basin-wide bedrock erosion rate for each time period, we first divided the sediment yield by the steadily decreasing contributing basin area (741 km^2 in 2005 (Rivera et al., 2007)), to obtain a sediment production rate. The sediment production rate was then converted to an equivalent volume of crystalline bedrock eroded by applying a glaciolacustrine sediment density of 1.8 g/cm^3 and a bedrock density of 2.7 g/cm^3 for the granites of the North Patagonian Batholith that underlie the glacier (SERNAGEOMIN, 2003).

Subaqueous landforms in Laguna San Rafael

The measured bathymetry of Laguna San Rafael (Fig. 2) is similar to what is shown on a bathymetric map of the lagoon published by the Chilean Navy in 1992 (Warren, 1993; Vieira, 2006). However, the sparse track coverage and minimal depth soundings used to generate the 1992 map missed several significant bathymetric highs and deep basins revealed by our more dense coverage of the lagoon. The bathymetric maps we generated identify two prominent, discontinuous, subaqueous moraines (Fig. 3B). The larger of the two moraines forms an almost continuous arc parallel to the Tempanos Moraine that bounds the lagoon. This moraine, approx. 3 km from the outer lagoon edge, corresponds to the ice front position in AD 1871 (Simpson, 1875) and 1898 (Steffen, 1910), suggesting it was deposited as the ice advanced to its maximum position at the end of the Little Ice Age. It is henceforth dubbed the LIA Moraine. The presence of such a moraine at the location of the ice front in AD 1871 also helps explain Simpson's description of ice cliffs ~100 m high (Simpson, 1875), which could only occur here if the terminus were grounded in shallow water. To the northwest this LIA Moraine is breached by a >60 m deep channel that aligns with the outlet to the Rio Tempanos, suggesting that during the last glacial advance the glacier and lagoon also drained through this river.

A second discontinuous, subaqueous moraine has formed around the mouth of the narrow outlet valley that crosses the range front. It forms two slightly arcuate spurs that extend westward from the range front along the valley sides, and is breached in the center by a deep, broad basin that slopes toward the inner fjord and current ice front. According to prior maps (e.g. Warren, 1993) and aerial photos, this moraine corresponds to the location of the AD 1935–1959 terminus standstill and is henceforth called the 1959 Moraine.

Between these two moraines, at ~100–120 m depth below lake level, is a broad basin. In addition, two small, discontinuous moraines can be found ~2 km east of the LIA Moraine. These were presumably formed by short-lived stability and deposition during the retreat phase between ~1900 and 1935.

Both the LIA and 1959 moraines can be traced onto land in the NE sector of the lagoon. The LIA Moraine emerges from the lagoon paralleling a doublet Moraine dated to 1910 (Winchester and Harrison, 1996). The 1959 Moraine aligns with low-amplitude ridges along a beach close to the park headquarters (see Fig. 2); these ridges were mapped as the ice-front position in 1959 by Lawrence and Lawrence (1959).

Sediment structures

Interpreting subsurface stratigraphy from sub-bottom and seismic reflection data uses the principal of seismic facies analysis. This method, although somewhat subjective, attempts to identify and group various reflection patterns (uniform horizontal reflectors, discontinuous, chaotic reflectors, etc.) observed in seismic records (e.g., Stoker et al., 1997, Stravers and Anderson, 1997; da Silva and Anderson, 1997). It is assumed that each pattern is characteristic of a particular type of sediment, geology or depositional environment, e.g. a continuous, thin reflector suggests fine-grained sediment deposited in a low-energy environment such as a glacial lake. The same pattern, but with a strong reflection (high amplitude) suggests a more compact, consolidated or coarse-grained material such as recessional outwash. Sediment deposited in a high-energy environment (e.g. proglacial delta) usually produce very strong reflections and the reflectors are often discontinuous. Areas of no subsurface penetration, with hyperbolic or arcuate patterns are characteristic of compact tills. In such fashion the seismic facies can be related to the inferred depositional environment.

Five distinct seismic facies were imaged in the subsurface sediments of Laguna San Rafael. The geologic interpretation of these seismic facies is:

a) Morainal deposits: moraines in the lagoon were primarily determined by morphology (see Fig. 4). Crests ranged from narrow (<200 m) and high (>40 m) (as in sample seismic image C in Fig. 4), to broad (>600 m) and double-crested (A in Fig. 4). The seismic reflection characteristic of the moraines are chaotic, with parabolic reflectors near the surface of the sediment package and a strong double reflector at the surface and the base of the moraine, suggestive of a hard, coarse or compacted layer. A seismically shallow, wavy and hummocky facies was imaged on the surface of some of the moraines (D in Fig. 4), indicative of slumping of the moraine crest. Deep within the moraines, laminations with low reflectivity can be found (best seen in D in Fig. 4). The moraines overlie one or more strong, low-angle reflectors, indicative of an unconformable, or compacted, base (described below).
b) Ice-proximal deposits: a seismic facies comprised of hummocky, wavy reflectors with many discontinuous, layered reflectors (E, F in Fig. 5); also seen on the surface of the moraines.
c) Ice-distal deposits: a semi-transparent, sub-horizontal to horizontal, strongly layered seismic facies (Fig. 6) that infills and drapes over dipping reflectors (e.g., H) and chaotic facies.
d) Unconformities/compacted surfaces: a low-angle, prominent, single or multiple reflector (Figs. 4–6), 30–150 ms below the sediment surface, mostly continuous across the lagoon west of the range front. In the inner fjord to the east (I, J in Fig. 6), the unconformable surface has considerable relief and the contact is defined by distinct parabolic reflectors, suggestive of a hard bedrock substrate. The strength of this reflector is inferred to represent compaction by glacial overriding. The semi-transparent, layered ice-distal deposits end abruptly at the contact with this surface in profiles where the contact is at an angle to the surface.
e) Infill/non-glacial deposits: a distinctly layered seismic facies, often onlapping the moraines or other protruding landforms at the edges of the lagoon (B in Fig. 4). The layers are sometimes overlain with a shallow chaotic facies, assumed to be recent slump deposits.

We interpret all sediments above the continuous, compacted surface (i.e., the flat, prominent reflector seen, for example, in E in

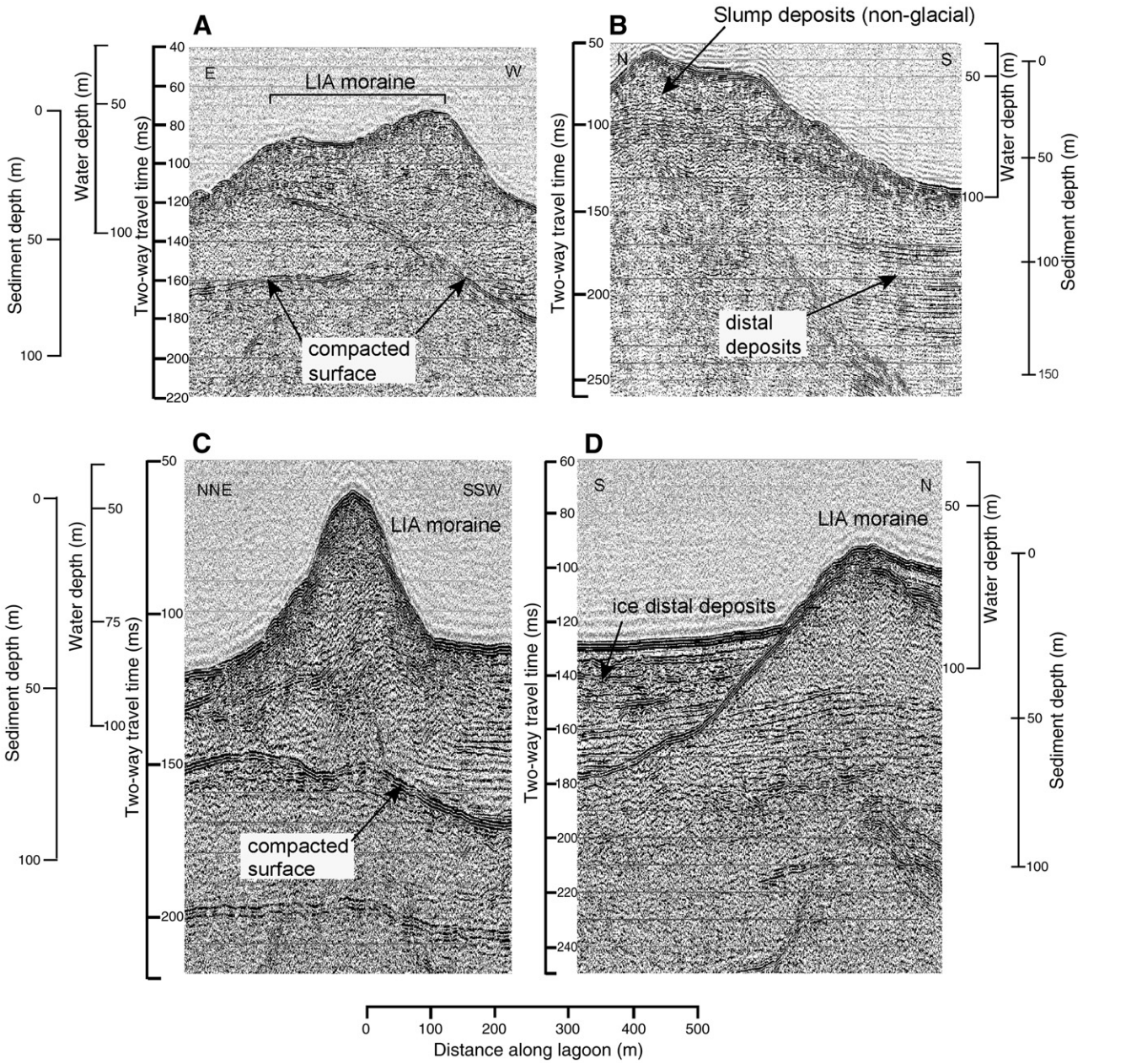

Figure 4. Representative seismic profiles of moraines and slump deposits in Laguna San Rafael. Many of the moraines overlay a strong, planar reflector, interpreted as the surface compacted by the previous glacier advance. A laminated facies onlaps the distal face of the moraines, suggesting rain out of distal fines as the glacier front pulled away from the moraine.

Fig. 5) to have been deposited once the ice started to retreat from the lagoon, with the exception of infill deposits near the edges of the lagoon that we interpret to be non-glacial in origin. This "postglacial" package includes the LIA and 1959 moraine deposits, as well as distal deposits between the LIA Moraine and the lagoon edge, that also overlie the flat reflector. The distribution and volume of sediments delivered by the glacier during its last advance and retreat were calculated using the thickness of the sedimentary package between the sediment surface and this underlying flat reflector, and mapped in Figure 3A. The locations of the major submerged landforms identified in the seismic reflection data are mapped in Figure 3B.

Moraine morphology and basin infill

The structure and size of the LIA Moraine match the Tempanos moraine complex that surrounds the lagoon (Winchester and Harrison, 1996; Glasser et al., 2006). The moraine exhibits a doublet crest in many places (A in Fig. 4), with slump deposits upfjord of the inner crest, and the outer crest prograding onto distal deposits. These features have been related to plowing of soft sediment by the glacier front (e.g., Powell, 1991). The structure of the LIA Moraine, with its sharp, high-amplitude crest (C in Fig. 4) overlapping and onlapping thick distal, layered deposits (D in Fig. 4), supports prior speculation that the glacier did not extend past its 1871 position during the last LIA advance (e.g., Casassa and Marangunic, 1987; Glasser et al., 2006).

Ice-distal sediments fill the 'moat', or depression, between the submerged LIA Moraine and the Tempanos Moraine that bounds the lagoon (H in Fig. 6). These distal fines onlap the outer flanks of the LIA Moraine (e.g., C, D in Fig. 4), but not the inner flank, suggesting that deposition of these fines was coeval with moraine construction. The thick laminated sediment package in the 'moat' also suggests that the

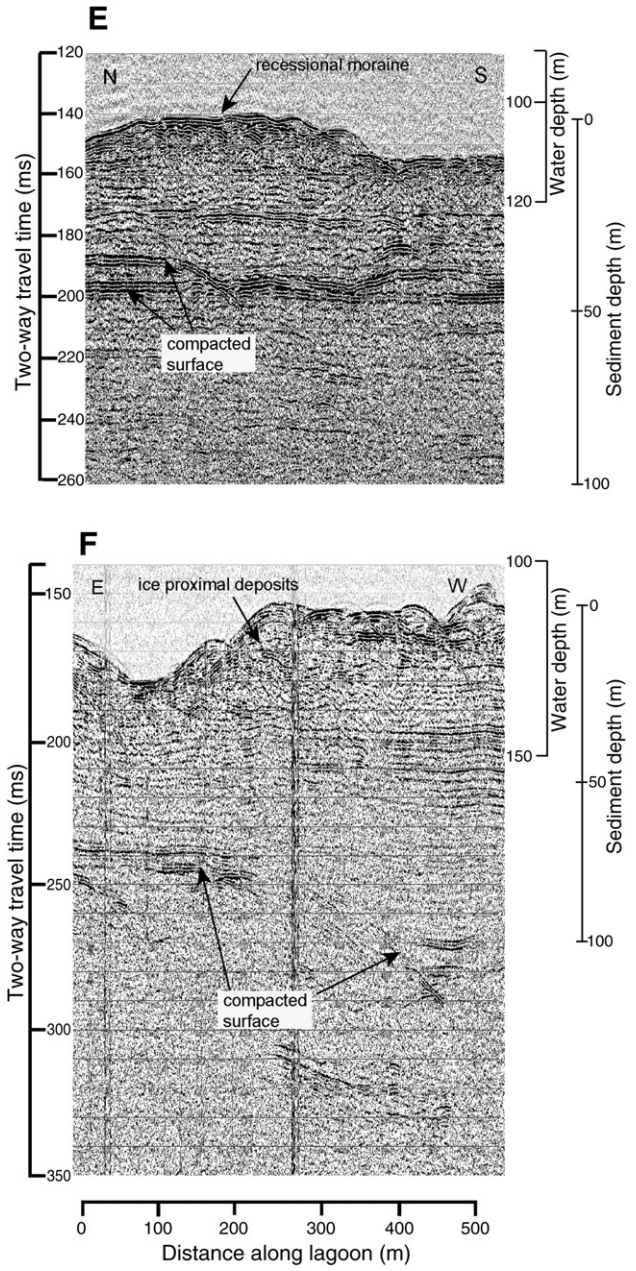

Figure 5. Seismic profiles of ice-proximal deposits in Laguna San Rafael. The ice-proximal facies is characterized by hummocky, chaotic reflectors overlying a distinct planar reflector.

terminus did not extend to the shores of the lagoon during the last advance. It is more likely that the terminus remained at the location of the LIA Moraine for several decades in order for these thick distal deposits to accumulate. Once the ice front started to retreat from its maximum stable position, the sediment delivered to the glacier front appears to have been trapped eastward of the LIA Moraine, filling the central basin (e.g., E in Fig. 5).

Two small, arcuate, hummocky deposits were mapped on top of the laminated facies located within 1–2 km east of the LIA Moraine (E in Fig. 5). These deposits, 15–20 m in amplitude, are presumed to be recessional moraines formed sometime around AD 1905. Their presence suggests that the terminus was grounded as it receded from its maximum LIA position. They also suggest that initial retreat was punctuated by temporary periods of stability that allowed enough sediment for moraine formation to be deposited (or reworked) at the ice front.

In the vicinity of the 1935–1959 standstill, hummocky ice-proximal deposits ~20 m thick were found, overlying >100 m of sub-horizontal layered sediments (F in Fig. 5). Unlike the LIA Moraine, which appears to have been deposited on top of a flat, compacted surface (Fig. 4), the 1959 Moraine appears to have been eroded out of a pre-existing layered deposit over 100 m thick (F in Fig. 5). In the center of the lagoon these layers are truncated at the breach between the two spurs of the moraine. Based on the distribution of this thick layered deposit at the edges of the central valley outlet, it appears that San Rafael Glacier did not splay as it flowed out from the valley that crosses the fault scarp.

Proglacial sediment reworking during the last advance

Between the LIA Moraine and the 1959 Moraine several prominent, sub-parallel reflectors were imaged within the sediment package (e.g., E in Fig. 5). The distinct, continuous trace of the reflectors suggests significant compaction of subglacial fines during the previous advance and retreat of the glacier front. The piedmont configuration of the terminus during the LIA advance and the low surface gradient of the glacier near the LIA terminus, evident from dated trimlines along the Andean front (Winchester and Harrison, 1996), suggest that there was low bed resistance and unconstrained flow during the last advance, indicating flow across a soft substrate. The presence of compact, horizontal reflectors is also consistent with erosion and plowing of a soft substrate during the last glacial advance, which would have contributed a significant amount of reworked material to the LIA Moraine and the moat beyond.

The significant relief (>120 m) between the ice-proximal deposits that crown the spurs of the 1959 Moraine and the broad, deep basin of the central valley outlet also suggests that during the last advance the glacier eroded over 100 m of soft sediment from the center of the channel, while leaving in place any deposits that filled the lagoon to the north and south of this central basin. This is a significant, but not unheard of, evacuation of sediment. For example, Taku Glacier, a temperate tidewater glacier similar in size and morphology to San Rafael Glacier and the only non-surge-type glacier currently advancing in southeast Alaska, has evacuated up to 200 m of unconsolidated, proglacial sediment since the start of its most recent advance at the end of the 19th century, at an erosion rate of ~2 m/a. (Motyka et al., 2006).

Subaerial sediment contribution

At the southeastern end of the lagoon, between the LIA and 1959 moraines, a thick (>40 m) distinct sequence of laminated and chaotic deposits was imaged (B in Fig. 4). This deposit suggests significant postglacial mass wasting of the range front, and delivery of debris directly from the hillslope to the lagoon. The volume of sediment in this deposit exceeds 0.33 km^3. Laminations in the deposit are inclined and onlap the 1959 Moraine and likely represent one or more deep-seated landslides, possibly triggered by the 1960 Valdivia earthquake (magnitude 9.5), an event that produced slip displacements as large as 20 m and significant coastal subsidence (intensity XI) in the region (Plafker and Savage, 1970). Earlier seismically-induced landslides into the lagoon are also possible; for instance, 2–2.5 m of subsidence was associated with an AD 1837 earthquake that flooded several km^2 of the forest bounding the lagoon (Simpson, 1875; Reed et al., 1988).

Subaerial sediments derived from the tectonically active range front may be a significant contributor to the overall sediment budget of the lagoon. Unfortunately, the slopes of the Andean range front are densely vegetated and inaccessible to overland travel. This makes it difficult to determine whether the fines unraveling from the slopes and accumulating in the lagoon derive from glacigenic material plastered to the hillslopes during the last advance, or from non-glacial, fault-weakened colluvium slumping into the lagoon. As the ultimate

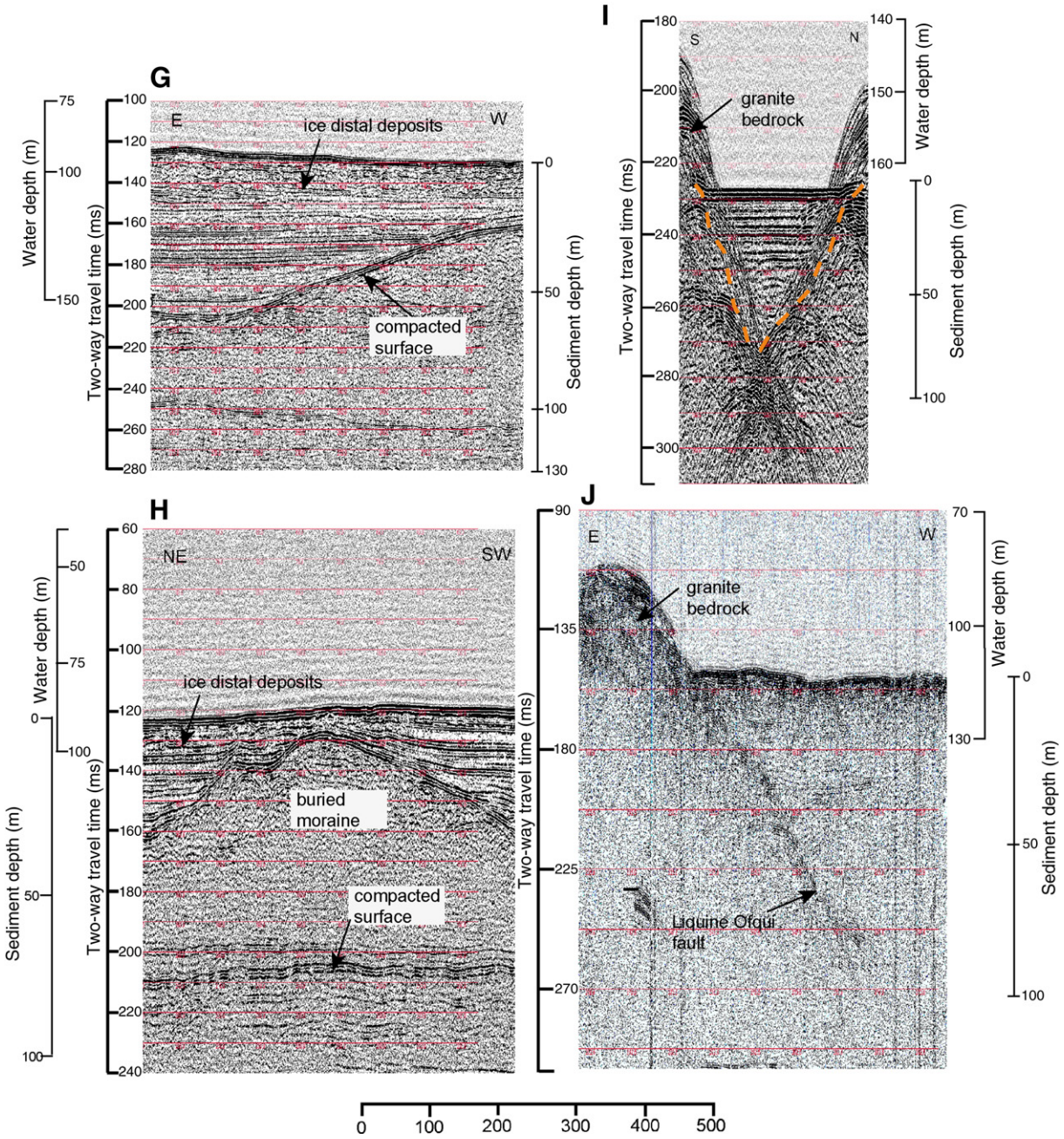

Figure 6. Seismic profiles of laminated sediments in Laguna San Rafael, interpreted as ice-distal deposits. The sub-horizontal laminated sediments overlap either a hummocky facies interpreted as ice-proximal deposits, or a distinct planar reflector, interpreted as the ice surface compacted by the prior advance. In some instances the distal fines drape buried moraines, reflecting standstills during recession. Panel J is a profile across the Liquiñe-Ofqui fault scarp. Panel I crosses an incised bedrock channel filled with ice-distal deposits, located in the inner fjord close to the terminus position in 1979. The right-hand side of the valley (dashed line) corresponds to the emergence of the valley wall above water line.

origin of these slide deposits is unclear, we chose to infer a non-glacial source and excluded all deltaic deposits from our estimates of glacial sediment yield.

Sediment yields and erosion rates during advance and retreat

The total volume of unconsolidated sediment in Laguna San Rafael, including all moraines, ice-proximal deposits, and ice-distal laminated sediments deposited since San Rafael Glacier last advanced during the mid-18th century exceeds 6 ± 1.3 km^3. The volume of sediment contained in the LIA Moraine is 1.5 ± 0.3 km^3 which is 25% of the total volume of postglacial sediment in the lagoon. This suggests that a) much of the sediment accumulated close to the terminus during the maximum standstill with little glaciofluvial evacuation during moraine deposition, and b) the LIA Moraine may contain a significant amount of sediment proglacial eroded from the lagoon itself and reworked by advancing ice. In contrast, the volume of sediment in the 1935–1959 moraine is only 0.2 ± 0.04 km^3, ~3% of the total, suggesting significant glaciofluvial evacuation and distal deposition of sediment during this standstill, a much shorter period of stability, and/or a significant decrease in the amount of sediment eroded and delivered by the glacier during this period.

Between AD 1871 and 1905, a period when the glacier started to recede into deeper water, 1.3 ± 0.5 km^3 of sediment accumulated in the lagoon. This estimate excludes the LIA Moraine itself, much of which was most likely deposited during the prior advance and standstill. The average sediment yield from San Rafael Glacier during this initial period of retreat was $3.9 \pm 1.4 \times 10^7$ m^3/a, corresponding to

a calculated average basin-wide bedrock erosion rate for the period 1871–1905 of 34 ± 13 mm/a. In contrast, 1.5 ± 0.5 km^3 of sediment accumulated between 1905 and 1921, and 0.77 ± 0.3 km^3 between AD 1921 and 1959 (including the standstill from 1935 to 1959); the average basin-wide glacial erosion rates during these periods increased to 68 ± 26 mm/a, then decreased to 18 ± 7 mm/a, respectively. These rates are as much as four times the erosion rate estimated for the glacier since 1959: 16 ± 5 mm/a. Hence, basin-wide erosion rates were greatest at the start of the most recent period of retreat, when the glacier pulled back from the LIA Moraine and retreated into deeper water, and have since been steadily decreasing throughout the past century (Fig. 7).

The thick deposits in the LIA Moraine and laminated fines that fill the distal moat beyond it account for 2.4 ± 0.9 km^3 of sediment. This is over one third of the total sediment volume in the lagoon, implying that significant erosion of the basin also occurred during the LIA advance and standstill. If we assume, to first order, that all of this material was primary bedrock eroded and entrained by San Rafael Glacier during this LIA advance, and does not include any unconsolidated material previously deposited in the lagoon and entrained by the advancing ice, then the total volume of sediment in the LIA Moraine and moat beyond would require over 2 m of bedrock eroded basin-wide over the period of advance and standstill. However, given that the last advance and standstill occurred over approximately 150–200 a, as suggested by the original maps of Laguna San Rafael in AD 1675 and 1871 (Araneda et al., 2007), then the average bedrock erosion rate (not including any reworking of proglacial or subglacial sediment) during the advance phase was at most 10 mm/a.

The presence of low-angle, compacted layers deep within the sediments throughout the basin and the deep channel eroded into the layered sediments in the center of the lagoon implies that there has also been significant entrainment and reworking of debris as the glacier advanced across the lagoon. Any distal fines deposited during and after the prior Holocene advance would have been easily remobilized by the advancing terminus and redeposited at the maximum extent of the LIA advance, and would therefore constitute a substantial portion of the sediments deposited in the LIA Moraine and distal moat (see Fig. 8). Although the total volume of reworked debris is hard to accurately determine since the pre-LIA bathymetry of the lagoon is not known, the >100 m of fines removed from the center of the lagoon suggests that this contribution must be at least 0.62 km^3, 1/4 of the sediment in the LIA Moraine and moat. Therefore, estimates of new material eroded from the entire glacial basin during the Little Ice Age advance and standstill are likely much lower, perhaps as low as 5–7 mm/a.

It is noteworthy that erosion rates during the advance phase of San Rafael's glacial cycle appear to be nearly an order of magnitude lower than during the retreat phase, contradicting the commonly held assumption that erosion rates should increase as a function of the amount of ice cover in the basin (e.g. Harbor and Warburton, 1993; Brozovic et al., 1997). That the San Rafael Glacier appears to have increased its erosional efficacy during retreat is not surprising, however, if we consider that the past century of warming has led to rapid glacier thinning and terminus retreat, which may in turn accelerate ice motion, as recently documented by outlet glaciers in Greenland and Alaska (Howat et al., 2005; Arendt et al., 2002), enhancing basal sliding and increasing rates of glacial erosion.

New glacial erosion vs. subglacial storage

The substantial volume of sediment that has accumulated over the past century of retreat at Laguna San Rafael suggests that the sediment yields we are measuring primarily reflect new bedrock erosion under the glacier, and not simply a change in the rate of evacuation of subglacial stores of sediments, sustained over decades. San Rafael Glacier occupies over 90% of its basin; therefore sediment contributions from paraglacial processes are negligible in this instance. The total volume of sediment delivered to the lagoon post-deposition of the LIA Moraine (i.e. ~1900–2005) is 3.5 km^3. The amount of sediment that could have been stored under or on top of San Rafael Glacier and remobilized over the past century to produce this significant volume could most likely be only a small fraction of this total. To attribute 3.5 km^3 of sediment solely to enhanced evacuation of subglacial sediment stores remobilized during retreat would necessitate the removal of a uniform layer of basal sediment >20 m thick from under the entire ablation area of the glacier, or >40 m thick

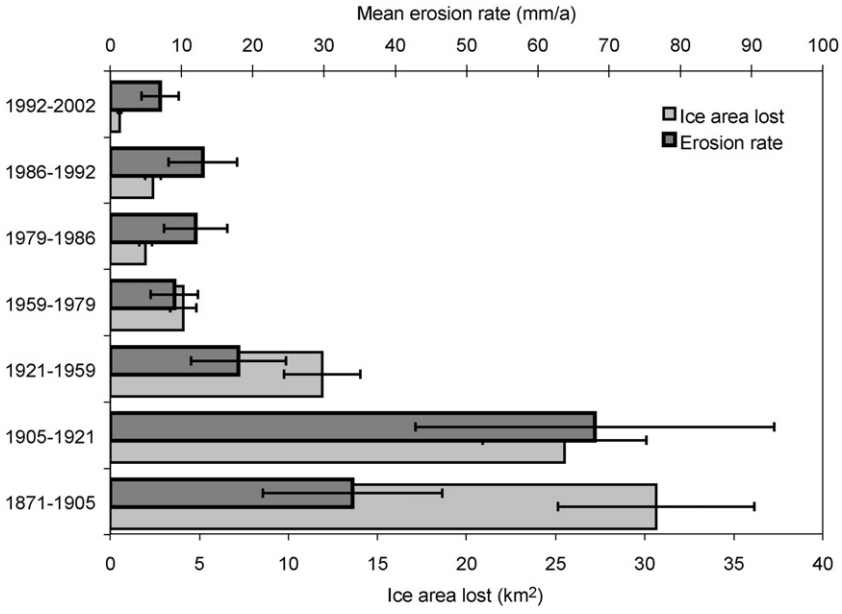

Figure 7. Rate of basin-averaged bedrock erosion (top axis) and loss of glacier terminus area (bottom axis) of San Rafael Glacier averaged over selected time intervals since the end of the Little Ice Age, synthesized from published terminus positions and sediment volume measurements. Error bars indicate compounded uncertainties in the terminus locations, associated sediment yields, and sediment-bedrock density ratios.

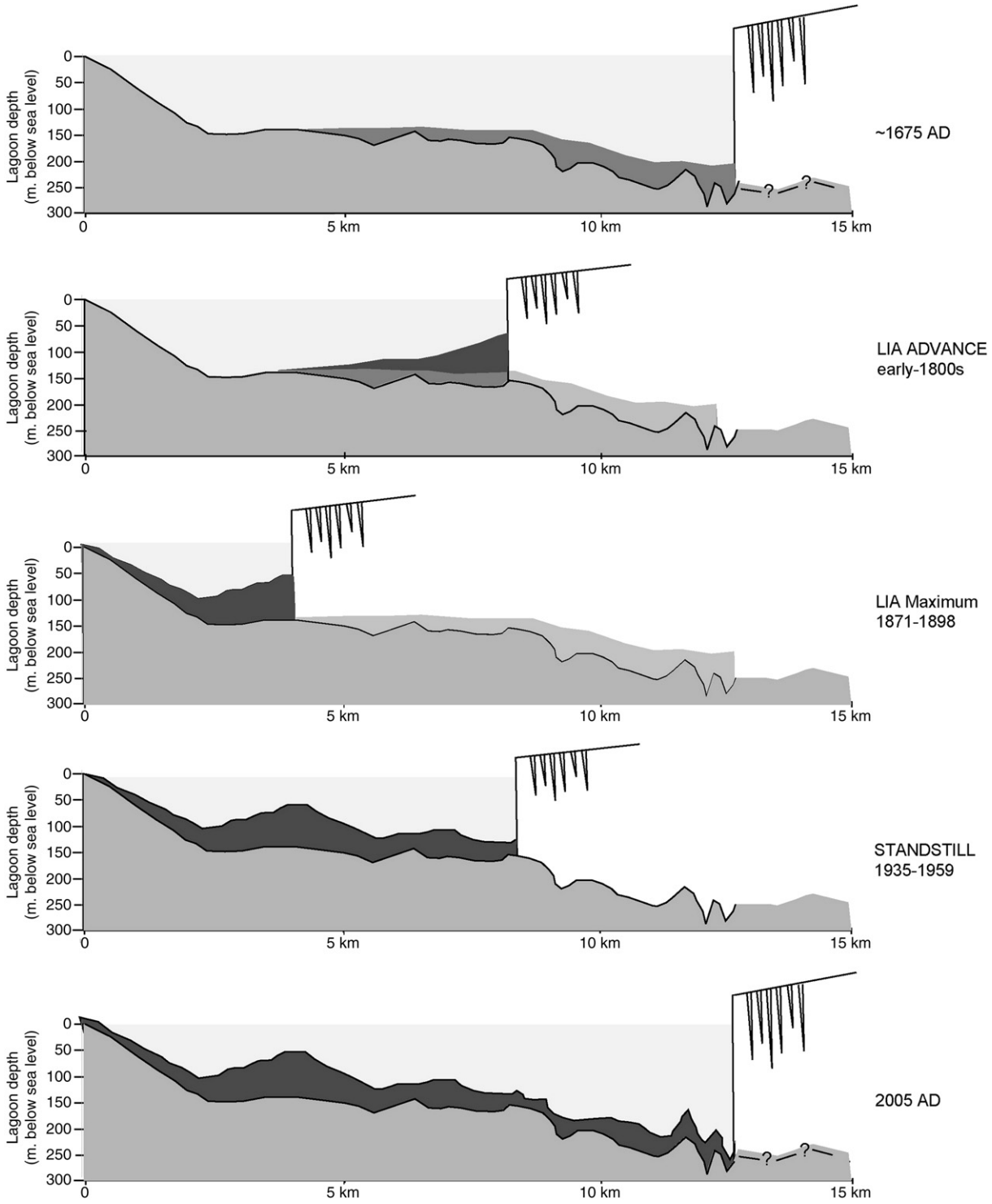

Figure 8. Cartoon interpretation of the Little Ice Age advance and retreat of San Rafael Glacier and the associated sedimentary sequences found in Laguna San Rafael. Proglacial, unconsolidated sediment deposited during and after the prior Holocene advance are in medium grey. The "postglacial" Little Ice Age sediment package is in dark grey.

from the fast moving ice tongue that cascades down from the icefield plateau. The characteristic thickness of basal debris, measured from boreholes that have penetrated temperate tidewater glaciers similar to San Rafael, is generally at most a few decimeters (Humphrey et al., 1993; Kamb et al., 1985). In other words, the sediment stores needed to produce the yields we are seeing from San Rafael Glacier are out of the realm of observed thicknesses of subglacial debris. Furthermore, this would preclude any bedrock erosion from having occurred over the past 100 a in this zone of fast ice flow by preventing sliding ice from having any direct contact with the underlying bed.

Implications for calving and landscape dynamics

The prominent compacted layers that underlie the LIA Moraine and extend eastward to the rangefront suggest that the piedmont lobe of San Rafael Glacier was grounded throughout its advance. The ice-proximal deposits above the compacted surface located 1–2 km east of the LIA Moraine suggest that the glacier was also grounded across its centerline as it started to retreat from its LIA position. The lack of proximal deposits in the deeper center of the basin upfjord of the recessional moraines suggest that the center of the piedmont lobe

may have floated for short periods of time during retreat. A floating tongue may have also buried a small recessional moraine in the southern part of the fjord with distal fines (see H in Fig. 6), while the northern edge of the piedmont remained grounded. There is little evidence, however, of widespread separation of the glacier from its bed that would indicate flotation driving collapse and rapid retreat.

The thick sequence of chaotic layered deposits along the rangefront at the eastern edge of the lagoon indicates significant unraveling of the fault scarp once the glacier receded mid-century. Along the scarp of the Liquiñe-Ofqui fault, a slump deposit >80 m thick (see Fig. 3a), which accumulated after 1935, mirrors the massive landslides observed near the termini of other rapidly retreating tidewater glaciers in tectonically active orogens (e.g., Meigs et al., 2006). The direct contribution of subaerial sediment to adjacent fjords and lagoons from changes in base level due to tectonic activity and/or the removal of a backstop as the glacier terminus retreats, thins and exposes oversteepened slopes can be substantial (e.g. Church and Ryder, 1972). The subaerial contribution can be particularly significant in tectonically active orogens where frequent seismic activity can enhance mass wasting and localize crustal and surface weakening. At Laguna San Rafael, these mass-wasting events contributed as much as 15% of the total volume of sediment in the lagoon.

The 6 km^3 of subaqueous Holocene age glacial sediment in Laguna San Rafael, adjacent to the icefield, highlights the importance of pinpointing the timing of sediment transfer from the orogen to the continental shelf in the evolution of active margins and evaluation of postglacial rebound. That hundreds of meters of glacially derived sediments can remain trapped in lagoons and fjords abutting the icefields suggests that much of the sediment produced during periods between major glaciations may collect at the rangefront, quite close to the source areas. This sediment often remains trapped in the overdeepened fjords and is not evacuated until the next major glaciation forces ice to extend out to the continental shelf, over 60 km to the west. The accumulation of vast volumes of sediment in close proximity to the glaciers and icefields that produce them may dampen any isostatic response that would be expected from the loss of ice following the end of glaciation. Modeled postglacial rebound rates of 14 mm/a and greater have been estimated in this region, based on ice volume lost since the Little Ice Age (Ivins & James, 2004). Extrapolating the total ice mass lost from San Rafael Glacier since the LIA using late 20th-century thinning rates measured by Rignot et al. (2003), the ice mass missing from this one glacier approaches 32 Gt. The 55Gt of glacimarine sediment delivered to this one outlet along the icefield margin, as well as the corresponding evacuation of this material from the glaciarized basin, would significantly confound postglacial rebound rates due to ice mass loss. The potential for a significant delay of 10^3–10^4 a between producing and mobilizing sediment from glaciated basins and depositing them beyond the continental margins needs to be considered both in models of landscape evolution and postglacial rebound, as well as in attempts to interpret sedimentary archives of exhumation in terms of climatic responses and glacial cycles.

Conclusion

Detailed investigation of the seabed and subsurface stratigraphy and geomorphology of Laguna San Rafael reveals an extensive sequence of glaciolacustrine deposits created during the last advance and subsequent recession of San Rafael Glacier into the lagoon. The precise timing of this advance, which formed a large subaqueous moraine in the outer portion of the lagoon, remains unknown, but most likely peaked during the mid- to late-19th century. The end of the Little Ice Age, sometime around AD 1871–1898, is used to bracket the centennial sediment yields out of the glacier. Basin-wide erosion rates from San Rafael Glacier have averaged 23 ± 9 mm/a since the Little Ice Age. These rates were much lower during the last advance and standstill, ~7 mm/a. Glacial erosion rates were highest at the start of the current phase of retreat, averaging 34 ± 13 mm/a between 1871 and 1905, and 68 ± 27 mm/a between 1905 and 1921, before dropping significantly in the latter half of the 20th century, reflecting changing ice dynamics and accelerated ice motion during rapid retreat.

This work highlights the value of collecting sub-bottom reflection data to calculate sediment volumes and document sequences of erosional and depositional events. The sub-bottom acoustic profiles are invaluable for interpreting the significant reworking of sediments by ice in the fjords, which need to be taken into account when using sediment volumes to estimate the efficiency of glacier erosion over the long term.

Acknowledgments

We thank Rosemary Vieira for help in the field and access to prior bathymetric data, the captain and crew of the M/V Petrel IV for access to Laguna San Rafael, John Anderson and Julia Wellner for help in collecting preliminary seismic profiles in 2005, and Brian Menounos and Neil Glasser for constructive and thorough reviews. This material is based upon work supported by the National Science Foundation under Grant OPP #03-338371. Andrés Rivera was partially funded by FONDECYT 1080320.

References

Araneda, A., Torrejón, F., Aguayo, M., Torres, L., Cruces, F., Cisternas, M., Urrutia, R., 2007. Historical records of San Rafael Glacier advances (North Patagonian Icefield): another clue to "Little Ice Age" timing in southern Chile? The Holocene 17 (7), 987–998.

Arendt, A.A., Echelmeyer, K.A., Harrison, W.D., Lingle, C.S., Valentine, V.B., 2002. Rapid wastage of Alaskan glaciers and their contribution to sea level rise. Science 297, 382–386.

Bart, P.J., Anderson, J.B., 1995. Seismic record of glacial events affecting the Pacific margin of the northwestern Antarctic Peninsula. In: Cooper, A.K., Barker, P.F., Brancolini, G. (Eds.), Geology and Seismic Stratigraphy of the Antarctic Margin, 68, pp. 75–95. Antarctic Research Series.

Brozovic, N., Burbank, D.W., Meigs, A.J., 1997. Climatic limits on landscape development in the northwestern Himalaya. Science 276, 571–574.

Casassa, G., Marangunic, C., 1987. Exploration history of the North Patagonian Icefield. Bulletin of Glacier Research 4, 163–175.

Cembrano, J., Hervé, F., Lavenu, A., 1996. The Liquiñe Ofqui fault zone: a long-lived intraarc fault system in southern Chile. Tectonophysics 259, 55–66.

Church, M., Ryder, J.M., 1972. Paraglacial sedimentation: a consideration of fluvial processes conditioned by glaciation. Geological Society of America Bulletin 83, 3059–3072.

da Silva, J.L., Anderson, J.A., 1997. Glacial marine seismic facies in a southern Chilean fjord. In: Davies, T.A., et al. (Ed.), Glaciated Continental Margins: an Atlas of Acoustic Images. Chapman & Hall, London, pp. 198–202.

Elverhøi, A., Svendsen, J.I., Solheim, A., Andersen, E.S., Milliman, J., Mangerud, J., Hooke, R.LeB., 1995. Late Quaternary sediment yield from the high Arctic Svalbard area. Journal of Geology 103 (1), 1–17.

Glasser, N.F., Jansson, K., Mitchell, W.A., Harrison, S., 2006. The geomorphology and sedimentology of the 'Tempanos' moraine at Laguna San Rafael, Chile. Journal of Quaternary Science 21 (6), 629–643.

Glasser, N.F., Jansson, K., Harrison, S., Rivera, A., 2005. Geomorphological evidence for variations of the North Patagonian Icefield during the Holocene. Geomorphology 71, 263–277.

Glasser, N.F., Harrison, S., Winchester, V., Aniya, M., 2004. Late Pleistocene and Holocene palaeoecology and glacier fluctuations in Patagonia. Global and Planetary Change 43, 79–101.

Harbor, J., Warburton, J., 1993. Relative rates of glacial and nonglacial erosion in alpine environments. Arctic and Alpine Research 25, 1–7.

Hay, W.W., Sloan, J.L., Wold, C.N., 1988. Mass/age distribution and composition of sediments on the ocean floor and the global rate of sediment subduction. Journal of Geophysical Research 93, 14933–14940.

Heusser, C.J., 1960. Late-Pleistocene environments of the Laguna San Rafael area, Chile. Geogaphical Reviews 50, 555–577.

Howat, I.M., Joughin, I., Tulacyk, S., Gogineni, S., 2005. Rapid retreat and acceleration of Helheim Glacier, east Greenland. Geophysical Research Letters 32, L22502.

Humphrey, N.F., Raymond, C.F., 1994. Hydrology, erosion and sediment production in a surging glacier: Variegated Glacier, Alaska, 1982–1983. Journal of Glaciology 40, 539–552.

Humphrey, N.F., Kamb, B., Fahnestock, M., Engelhardt, H., 1993. Characteristics of the bed of the lower Columbia Glacier, Alaska. Journal of Geophysical Research 98 (B1), 837–846.

Ivins, E.R., James, T.S., 2004. Bedrock response to Llanqihue Holocene and present-day glaciation in southernmost South America. Geophysical Research Letters 31, L24613. doi:10.1029/2004GL021500.

Kamb, B., Raymond, C.F., Harrison, W.D., Engelhardt, H., Echelmeyer, K.A., Humphrey, N., Brugman, M.M., Pfeffer, T., 1985. Glacier surge mechanism: 1982–1983 surge of Variegated Glacier, Alaska. Science 227 (4686), 469–479.
Kondo, H., Yamada, T., 1988. Some remarks on the mass balance of the terminal-lateral fluctuations of San Rafael Glacier, the Northern Patagonia Icefield. Bulletin of Glacier Research 6, 55–63.
Koppes, M.N., 2007. Glacier erosion and response to climate, from Alaska to Patagonia., University of Washington: Ph.D. thesis, 222 pp.
Lagoe, M.B., Eyles, C.H., Eyles, N., Hale, C., 1993. Timing of late Cenozoic tidewater glaciation in the far North Pacific. Geological Society of America Bulletin 105, 1542–1560.
Lawrence, D.B., Lawrence, E.G., 1959. Recent Glacier Variations in Southern South America. Technical Report, Office of Naval Research. American Geographical Society, New York, p. 39.
Masiokas, M., Rivera, A., Espizua, L., Villalba, R., Delgado, S., Aravena, J.C., 2009. Glacier fluctuations in extratropical South America during the past 1000 years. Palaeogeography Palaeoclimatology, Paleaoecology 281, 242–268.
Mayr, C., et al., 2007. Holocene variability of the Southern Hemisphere westerlies in Argentinean Patagonia (52S). Quaternary Science Reviews 26, 579–584.
Meigs, A., Krugh, W.C., Davis, K., Bank, G., 2006. Ultra-rapid landscape response and sediment yield following glacier retreat, Icy Bay, southern Alaska. Geomorphology 78, 207–221.
Mercer, J.H., 1976. Glacial history of southernmost South America. Quaternary Research 6, 125–166.
Motyka, R.J., Truffer, M., Kuriger, E.M., Bucki, A.K., 2006. Rapid erosion of soft sediments by tidewater glacier advance: Taku Glacier, Alaska, USA. Geophysical Research Letters 33, L24504. doi:10.1029/2006GL028467.
Muller, E.H., 1960. Glacial chronology of the Laguna San Rafael area, Southern Chile. Bulletin of the Geological Society of America 71, 2106.
Peizhen, Z., Molnar, P., Downs, W.R., 2001. Increased sedimentation rates and grain sizes 2–4 Myr ago due to the influence of climate change on erosion rates. Nature 410, 891–897.
Plafker, G., Savage, J.C., 1970. Mechanism of the Chilean earthquakes of May 21 and 22, 1960. Geological Society of America Bulletin 81, 1001–1030.
Powell, R.D., 1991. Grounding-line systems as second-order controls on fluctuations of tidewater termini of temperate glaciers. In: Anderson, J.B., Ashley, G.M. (Eds.), Glacial Marine Sedimentation; Paleoclimatic Significance, Geological Society of America Special Paper 261, pp. 75–94.
Reed, D., Wood, R., Best, J., 1988. Earthquakes, rivers and ice: scientific research at the Laguna San Rafael, Southern Chile, 1986. The Geographical Journal 154, 392–405.
Rignot, E., Rivera, A., Casassa, G., 2003. Contribution of the Patagonia Icefields of South America to sea level rise. Science 302, 434–437.
Rignot, E., Forster, R., Isacks, B., 1996. Interferometric radar observations of Glaciar San Rafael, Chile. Journal of Glaciology 42 (141), 279–291.
Rivera, A., Benham, T., Casassa, G., Bamber, J., Dowdeswell, J., 2007. Ice elevation and aerial changes of glaciers from the Northern Patagonian Icefield, Chile. Global and Planetary Change 59, 126–137.
SERNAGEOMIN, 2003. Mapa Geológico de Chile: versión digital. Servicio Nacional de Geología y Minería, Publicación Geológica Digital, No. 4 (CD-ROM, versión1.0, 2003). Santiago.
Simpson, E.M., 1875. Esploraciones hechas por la corbeta Chacbuco. Anuario Hidrografico de la Marina de Chile 1, 3–166.
Steffen, H., 1910. Viajes de esploracion y estudio en la Patagonia Occidental, 2. Imprenta Cervantes, pp. 1892–1902.
Stoker, M.S., Pheasant, J.B., Josenhans, H., 1997. Seismic methods and interpretation. In: Davies, T.A., et al. (Ed.), Glaciated Continental Margins: an Atlas of Acoustic Images. Chapman & Hall, London, pp. 9–26.
Stravers, J.A., Anderson, J.A., 1997. A late glacier readvance moraine in the central Chilean fjords. In: Davies, T.A., et al. (Ed.), Glaciated Continental Margins: an Atlas of Acoustic Images. Chapman & Hall, London, pp. 40–41.
Van der Veen, C.J., 2002. Calving glaciers. Progress in Physical Geography 26, 96–122.
Vieira, R., 2006. Interpretação integrada de sísmica de alta-resolução e da morfologia submarina da Costa de Fiordes da Patagônia Central-Chile. PhD thesis, UFRGS, Porto Alegre, Brazil. 181 pp.
Vorren, T.O., Richardsen, G., Knutsen, S.M., Henriksen, E., 1991. Cenozoic erosion and sedimentation in the western Barents Sea. Marine and Petroleum Geology 8 (3), 317–340.
Warren, C.R., 1993. Rapid recent fluctuations of the calving San Rafael Glacier, Chilean Patagonia: climatic or non-climatic. Geografiska Annaler 75 A (3), 111–125.
Winchester, V., Harrison, S., 1996. Recent oscillations of the San Quintin and San Rafael Glaciers, Patagonian Chile. Geografiska Annaler 78 A (1), 35–49.